J. C. Nolasco, J. W. Ryan, M. Rodriguez, A. Castro-Carranza, J. L. Maldonado, G. Ramos-Ortiz, O. Barbosa-Garcia, J. Gutowski, E. Palomares, J. Parisi

Organoboron donor-π-acceptor chromophores for small-molecule organic solar cells

Recommended Citation (primary publication/Version of Record) incl. DOI:

Nolasco, J.C., Ryan, J.W., Rodríguez, M. et al. Organoboron donor-π-acceptor chromophores for small-molecule organic solar cells. J Mater Sci: Mater Electron 29, 16410–16415 (2018). https://doi.org/10.1007/s10854-018-9732-6

Organoboron donor-π-acceptor chromophores for small-molecule organic solar cells

J. C. Nolasco[1,2] · J. W. Ryan[3] · M. Rodríguez[4] · A. Castro-Carranza[5] · J. L. Maldonado[4] · G. Ramos-Ortiz[4] · O. Barbosa-Garcia[4] · J. Gutowski[5,7] · E. Palomares[6,8] · J. Parisi[1]

Abstract

We introduce the use of facilely synthesizable and low-bandgap boron chromophores as donors in planar heterojunction solar cells. We show that simple changes in the compositional properties of these molecules can improve the performance of the devices. A simultaneous grafting of NO_2 acceptor and $N(Et_2)$ donor groups into the molecule core causes an increase in efficiency of almost 50%. Such enhanced efficiency is mainly due to a higher photocurrent. The origin of this phenomenon is investigated.

1 Introduction

Organic solar cells (OSCs) are promising for future low-cost and environmentally friendly renewable energy sources. Recent progress has resulted in efficiency values of around 15% for both polymer:fullerene bulk heterojunction (BHJ) devices and small-molecular weight compound OSCs (SMOSCs) [1–4]. The advantages of using small-molecule donors in comparison to polymers are numerous, e.g., they allow for applying facile synthesis and purification methods, are mono-disperse, and devices can be fabricated via thermal or solution processing.

Besides the efficiency enhancement in OSCs, other factors must be considered such as stability and cost.

Organoboron chromophores are interesting in this respect as they are readily synthesizable, and their electronic properties are extremely well tunable. The high versatility of boron chemistry has resulted in interesting applications of boron compounds, such as medical applications [5], p–n junctions [6], solar cells [7], and photonic applications. Regarding the optical properties of organoboron molecules, systematic studies of nonlinear optical effects for different boron complexes have been carried out [8, 9]. The results of such studies indicate unique characteristics of boron compounds, such as high absorption coefficients at large wavelength, a planar π-conjugate core, and an ordered packing structure in solid films [9]. These characteristics make organoboron derivatives promising donor materials for photovoltaic applications.

Recently, a boronsubphthalocyanine chloride has been used in OSCs [10], further, polymers based on BODIPY

✉ J. C. Nolasco
 jairo.cesar.nolasco.montano@uni-oldenburg.de;
 jairo.nolasco@comunidad.unam.mx

1 Energy and Semiconductor Research Laboratory, Department of Physics, Carl von Ossietzky University of Oldenburg, Oldenburg 26111, Germany

2 Science of Sustainable Materials, National School of Higher Studies Unit Morelia, National Autonomous University of Mexico (ENES Morelia UNAM), 58190 Morelia, Mexico

3 International Center for Young Scientists (ICYS), National Institute for Materials Science (NIMS), 1-1 Namiki, Tsukuba, Ibaraki 305-0044, Japan

4 Research Group of Optical Properties of Materials (GPOM), Centro de Investigaciones en Óptica A.C., A.P. 1-948, 37000 León, Guanajuato, Mexico

5 Institute of Solid State Physics, Semiconductor Optics, University of Bremen, 28359 Bremen, Germany

6 Institute of Chemical Research of Catalonia (ICIQ), 43007 Tarragona, Spain

7 MAPEX Center of Materials and Processes, University of Bremen, Bremen, Germany

8 Institució Catalana de Recerca i Estudis Avançats (ICREA), 08010 Barcelona, Spain

backbone cores have been reported for photovoltaic applications [11]. However, the synthesis of these compounds, in particular, that used to obtain polymers, is complicated, and it can be difficult to tailor their optoelectronic properties [12]. Here, we introduce the use of three original borinates as donors in OSCs as a low-cost alternative due to their facile synthesis and ease of functionalization.

2 Sample preparation and experimental procedures

2.1 Organoboron solar cell fabrication

Figure 1 shows the molecular structure of the three boron compounds used in this study. The molecules possess a common R_2BON core with extended π conjugation stemming from the nitrogen. The π-conjugated chain is capped with a nitrogen donating group (alkylamine). In this work, we study the effect of two compositional changes in the initial molecule (B1) on the solar cells performance, first, the effect of the addition of an NO_2 acceptor group (B2), and second, the effect of changing the dimethyl donating group with a diethyl one, i.e., $N(Me_2)$ with $N(Et_2)$ (B3). The synthesis of the boron compounds was achieved by a simple two-step process, i.e., first, the ligand (π-backbone) was synthesized by condensation reaction between respective amine and cinnamaldehyde derivatives by using methanol as a solvent, at the end of reaction time the imine products were purified by filtration technique. And second, the reaction of these ligands with diphenylboronic acid followed, specifically, boron complexation for ligand was carried out in ethyl acetate as a solvent at room temperature. The borinates obtained were washed with hexane and ethyl acetate:hexane (1:9) mixture to remove the residual starting materials. This methodology includes less synthetic steps and easier purification process than polymerization or croos-coupling reactions which are commonly used to prepare photovoltaic materials [9]. Their chemical structure and mass spectrum were verified by magnetic resonance and mass spectroscopy, respectively (see the Supporting Information).

Planar heterojunction solar cells were fabricated possessing the device structure ITO/MoO_3 (8 nm)/borinate (30 nm)/ C_{60} (40 nm)/BCP (8 nm)/Al (100 nm). The devices studied here employ a bilayer architecture to keep the analysis as simple as possible compared to the BHJ devices which can include additional contact effects, i.e. the donor (borinate)/ cathode (Al) junction, due to the nanomorphology of the blend [13]. Therefore, the bilayer architecture allows for a better comparison of the impact of the different molecular structures on the performance of the devices. The ITO substrates (Psiotec, 5 Ω/square) were first sonicated in acetone, followed by two cycles of sonication in iso-propanol, with each cycle lasting 15 min. Following this step, the substrates were treated with UV/O_3 prior to evaporation of MoO_3. Next, the boron compounds were deposited by spin coating the solutions on the MoO_3 coated ITO/glass substrate (1 mg/ml solution in $CHCl_3$). Subsequently, C_{60} (40 nm), BCP (8 nm), and Al (100 nm) were evaporated at a base pressure not exceeding 1×10^{-6} mbar. The devices possess an active area of 0.09 cm^2 and were studied under standard conditions (AM 1.5 G solar spectrum, 100 mW/cm^2).

2.2 Electrical and optical characterization

To analyze the electrical characteristics of the devices based on the three boron compounds, current density–voltage (J–V) measurements were carried out by using a Keithley 2400 power source at room temperature and under air conditions. For the characteristics under illumination, a 150 W xenon lamp from ABET Instruments with an incident light power of 100 mW/cm^2 was used.

The optical absorption spectra were measured with an Ultraviolet–Vis spectrophotometer (UV-2101PC, Shimadzu Corporation), and cyclic voltammetry (CV) was performed using a CH Instruments Potentiostat/Galvanostat Model 600D C series with a slow scan rate of 5 mV/s. The charge collection was quantified by incident photon-to-current efficiency (IPCE) measurements using a home-made set-up consisting of a 150 W Oriel xenon lamp, a motorized monochromator, and a Keithley 2400 digital source meter.

Fig. 1 Molecular structures of boron compounds
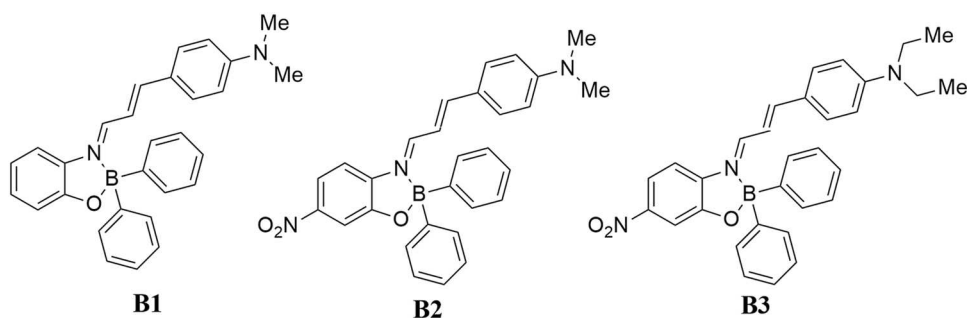
3 Results and discussion

Figure 2 shows the J–V characteristics of devices made by using each one of the above mentioned donor molecules (borinates B1, B2, B3, see Fig. 1). In Table 1, their photovoltaic parameters are given.

As it can be seen from Table 1, the open-circuit voltage (V_{oc}) and the fill factor differ slightly among the cells. The photocurrent density increases more significantly for B3 devices, leading to efficiency values of around 1%. It should be emphasized that, considering the simplicity of these boron compounds, our result is convincing with respect to those obtained for other more elaborated molecules such as boron subphthalocyanine chloride and polymers based on BODIPY's, which have resulted in efficiency values of 3 and 2%, respectively, in BHJ solar cells which are expected to provide higher efficiency with regard to the bilayer architecture, due to an increase of donor–acceptor interfacial areas [10, 11]. Suggestions on how to improve our device performance will be discussed later.

To elucidate the origin of the differences in the photovoltaic parameters among the solar cells fabricated, the optoelectronic properties of the compounds and the charge collection in the devices were investigated. Figure 3 shows the thin-film absorption coefficient spectra for each of the borinates presented in this study. The films were deposited using the same conditions as used for the devices. Looking at B1 firstly, which lacks the NO_2 acceptor group, we see that it absorbs between 400 and 650 nm, with a maximum peak centered around 520 nm. Addition of the NO_2 group induces a red-shift of the whole absorption feature for B2 and B3,
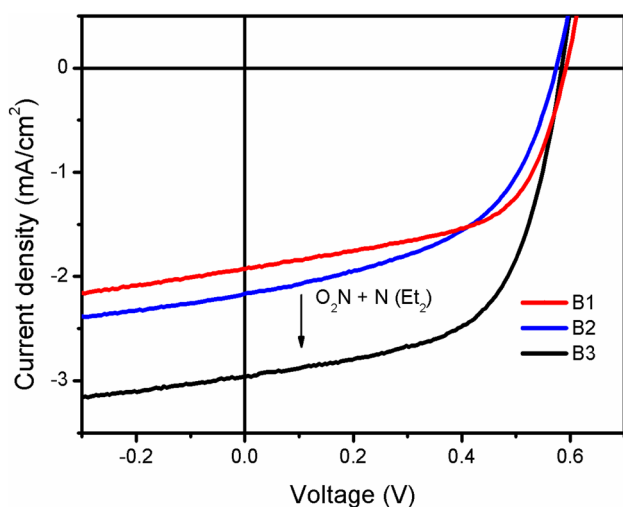
Table 1 Photovoltaic parameters of planar solar cells based on boron compounds

Boron compound	V_{oc} (V)	J_{sc} (mA/cm^2)	FF	PCE (%)
B1	0.59	1.93	0.57	0.65
B2	0.57	2.16	0.50	0.63
B3	0.58	2.95	0.59	1.02

extending the absorption profile up to 700 nm. Extending the alkyl chain on the terminating nitrogen electron-donating group, i.e., replacing NMe_2 by NEt_2, provides a significant enhancement in the absorption intensity of the thin films, as well as a larger coverage of the solar spectrum. Considering that, in general, the absorption intensity is directly proportional to the material´s distribution of states (where electronic transitions occur), and that it depends on the microstructure of the films in organic semiconductors [14], it is suggested that the B3 film possesses a larger amount of states which is attributed to the insertion of a strong donor group (NEt_2) into the molecule core. Further, the molar absorption coefficients of the compounds in solutions (concentration of 1×10^{-5} M in chloroform) were determined, see the spectra included as inset in Fig. 3. Although the peaks of the three compounds are centered around similar energy values as for the solid films, their intensity changes. This phenomenon is attributed to a structural change in the films. The two-peak absorption spectrum observed for B3 becomes more visible in the thin films and has been attributed to an increase of the material's trap states due to a molecular aggregation [15]. This aggregation can be detrimental to the device performance, particularly in a bulk hetero-junction structure since
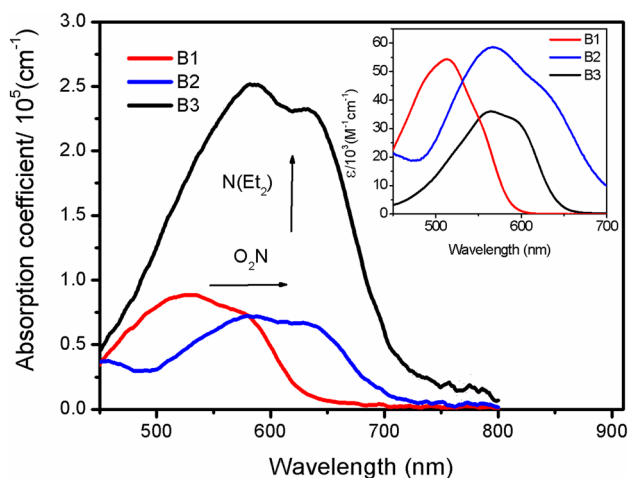

Fig. 2 J–V curves of solar cells with the structure ITO/MoO$_3$/borinate (B1, B2, B3)/C$_{60}$/BCP/Al under illumination with 100 mW/cm^2 AM 1.5 G

Fig. 3 Absorption coefficient of the boron compounds in solid thin films and in solutions (inset)

a bicontinuous interpenetrating network is desirable in this case [16–18].

The HOMO and LUMO levels were determined from the measured electrochemical onset potentials, as previously described in Refs. [19, 20]. The electrochemical band gap, shown in Table 2, was calculated as HOMO–LUMO. The optical band gap was also determined from the absorption spectra using a Tauc plot [21], Fig. 4.

We found that insertion of the NO_2 acceptor group into the boron molecule increases the LUMO level by approximately 0.4 eV and, consequently, reduces the bandgap E_g for the B2 and B3 compounds. E_g values around 1.6 eV were obtained for B2 and B3. These values are comparable to the one for PCE-10 semiconductor, which has been used in tandem OSCs [1]. The change in the LUMO levels of B2 and B3 explains the red-shift of their corresponding absorption maxima as observed in Fig. 3. The reduction of E_g by addition of acceptor groups is a strategy in organic semiconductors [12]. It yields more delocalized electrons due to a favourable molecular stacking [16]. An alternative novel strategy is the insertion of boron-nitrogen coordination bonds into conjugated polymers which has been used to downshift its LUMO and HOMO energy levels [22, 23]. It has been demonstrated that such polymers can be used as acceptors in relative efficient OSCs [24, 25]. The considerable change in E_g observed here results in relatively large shifts of both absorption bands of the molecules, illustrating the excellent optical tunability of these molecules due to subtle changes in the molecular structure. Further, the drastic enhancement of the absorption efficiency for B3 underscores the impact of such molecular structure changes. The electrochemical and optical bandgaps E_g, as given in Table 2, show a convincing agreement.

Further, in OSCs, V_{oc} is related to the energy levels of the molecules. In case V_{oc} is not predominantly affected by recombination in the contacts [13], it has been proposed that it is proportional to the difference of the HOMO of the donor and the LUMO of the acceptor [26]. The LUMO level of C_{60} (acceptor), which is common for all devices studied here, has been reported to amount to 4 eV [27]. The little differences in the HOMO energy observed for the three types of molecules and in V_{oc} after their insertion in the solar cells studied, respectively (see Tables 2, 1, respectively), are
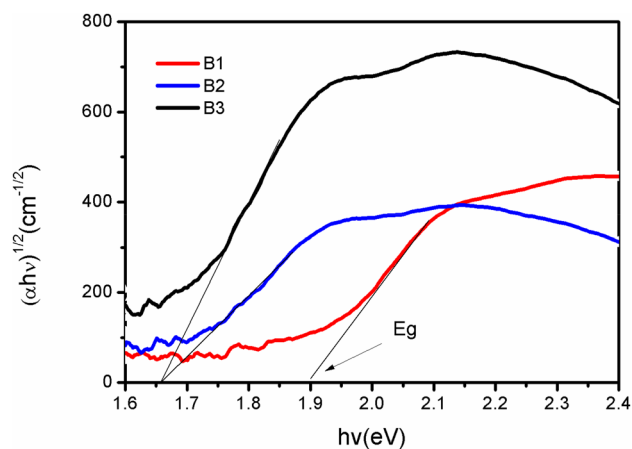

Fig. 4 Tauc plot of the absorption spectra of the boron compound films

consistent with such a trend. The LUMO–LUMO offsets of C_{60} and borinates are well above the empirical value of 0.3 eV required for charge separation [14].

Figure 5 shows the IPCE measurements performed for the three different devices. The absorption in the wavelength region around 470 nm has been typically attributed to C_{60} [10, 11]. The longer wavelength region, around 600 nm, corresponds to boron compounds (Fig. 3). As we can see in Fig. 5, the largest photo conversion efficiency across the entire spectrum is obtained for B3, and the biggest difference between the device IPCEs is found in the region in which the organoboron donors absorb. This trend is in good agreement with the observed absorption coefficient spectra of the simple films in Fig. 3. This result indicates that the red-shifted and higher absorption coefficient, which is due to the corresponding donor group change, observed for the
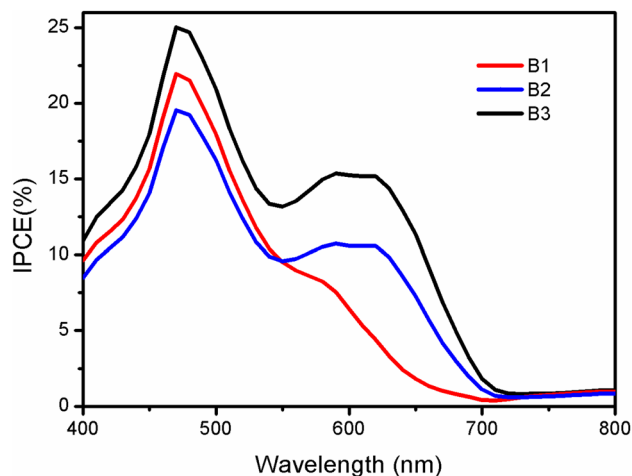
Table 2 Energy levels of boron compounds

Boron compound	HOMO (eV)	LUMO (eV)	$E_{g\text{-elec}}$ (eV)	$E_{g\text{-opt}}$ (eV)
B1	5.22	3.18	2.03	1.90
B2	5.22	3.66	1.56	1.66
B3	5.30	3.58	1.72	1.66

Electrochemical band gap ($E_{g\text{-elec}}$) and optical band gap ($E_{g\text{-opt}}$)

Fig. 5 Incident photon-to-current efficiency (IPCE) of the solar cells based on the three boron compounds

devices containing B3 is the main cause of the highest photocurrent generated in these devices. This result is in agreement with the one observed for larger molecules, it is the increment of photocurrent with the introduction of acceptor groups [11, 28].

In addition, considering that the C_{60} layer is the same for all devices and that the IPCE spectrum is governed by both, materials' light absorption and devices' charge collection, the following is suggested: (i) the relatively slight difference at the C_{60} region in Fig. 5 indicates that a better collection of the charges generated in the C_{60} film is occurring for the B3 device; and (ii) the reduction of the second peak of the B3 spectrum, when qualitatively comparing Figs. 3 and 5, may be due to a relatively poor device collection of the charges generated in the B3 film. Thus, the achievement of the largest fill factor for B3 devices indicates that the first phenomenon dominates, although this is not a striking effect. Further structural characterization must be done in both the thin films and the complete devices prepared with the borinates to study the effect of their structural properties on the charge collection in solar cells.

As future prospect, an improved molecular design using more elaborated donor and acceptor groups may lead to a more striking increase of the photocurrent. The still low IPCE efficiency values in Fig. 5 and, consequently, low photocurrent values for boron compound solar cells suggest that there exists an important margin to improve the device performance, e.g., by optimizing the thickness of the active films and testing other interlayer materials to reduce resistance effects, and thus to increase charge collection. Finally, it is expected that employment of the molecules in a bulk-heterojunction structure with a soluble fullerene derivative may improve the device performance due to an increase of donor–acceptor interfacial areas. In this case the active layer morphology should be carefully optimized [16–18].

4 Conclusions

The results obtained in this study clearly demonstrate that boron chromophores are good candidates to be applied in solar cell technology. We conclude that addition of NO_2 and $N(Et_2)$ substituents to the bare borinate molecule results in a red-shift of its absorption spectrum due to an increment in its LUMO level and an increment of its absorption coefficient; and, thus, in an improvement of the photocurrent in solar cells containing these modified molecules.

References

1. X. Che, Y. Li, Y. Qu, R. Forrest, Nat. Energy **3**, 422 (2018)
2. H. Zhang, H. Yao, J. Hou, J. Zhu, J. Zhang, W. Li, R. Yu, B. Gao, S. Zhang, J. Hou, Adv. Mater. **30**, 1800613 (2018)
3. H. Li, Z. Xiao, L. Ding, J. Wang, Sci. Bull. **63**, 340 (2018)
4. Z. Xiao, X. Jia, L. Ding, Sci. Bull. **62**, 1562 (2017)
5. M.F. Hawthorne, M.W. Lee, J. Neurooncol. **62**, 33 (2003)
6. F. Algi, A. Cihaner, Org. Electron. **10**, 453 (2009)
7. J.F. Salinas, J.L. Maldonado, G. Ramos-Ortíz, M. Rodríguez, M.A. Meneses-Nava, O. Barbosa-García, R. Santillan, N. Farfán, Sol. Energy Mater. Sol. Cells. **95**, 59 (2011)
8. M. Rodriguez, R. Castro-Beltran, G. Ramos-Ortiz, J.L. Maldonado, N. Farfán, O. Dominguez, J. Rodriguez, R. Santillan, M.A. Meneses-Nava, O. Barbosa-García, J. Peon, Synth. Met. **159**, 1281 (2009)
9. M. Rodríguez, J.L. Maldonado, G. Ramos-Ortiz, J.L. Lamère, P.G. Lacroix, N. Farfán, M.E. Ochoa, R. Santillan, M.A. Meneses, O. Nava, K. Barbosa-Garcia, Nakarani, New J. Chem. **33**, 1693 (2009)
10. R. Pandey, A.A. Gunawan, K.A. Mkhoyan, R.J. Holmes, Adv. Funct. Mater. **22**, 617 (2012)
11. B.S. Kim, B. Ma, V.R. Donuru, H. Liu, J.M.J. Fréchet, Chem. Commun. **46**, 4148 (2010)
12. G.E. Morse, M.G. Helander, J. Stanwick, J.M. Sauks, A.S. Paton, Z.H. Lu, T.P. Bender, J. Phys. Chem. C **115**, 11709 (2011)
13. J.C. Nolasco, G. Ramos-Ortiz, J.L. Maldonado, O. Barbosa-García, B. Ecker, E. von Hauff, Appl. Phys. Lett. **104**, 43308 (2014)
14. R. Noriega, J. Rivnay, K. Vandewal, F.P.V. Koch, N. Stingelin, P. Smith, M.F. Toney, A. Salleo, Nat. Mater **12**, 1038 (2013)
15. D.A. Seanor, *Electrical Properties of Polymers* (Academic Press, Inc., London, 1982), p. 70
16. Z. Liu, L. Zhang, M. Shao, Y. Wu, D. Zeng, X. Cai, J. Duan, X. Zhang, X. Gao, Appl. Mater. Interfaces **10**, 762 (2018)
17. S. Wen, Y. Wu, Y. Wang, Y. Li, L. Liu, H. Jiang, Z. Liu, R. Yang, ChemSusChem **11**, 360 (2018)
18. Z. Liu, Y. Wu, H. Jiang, L. Zhang, D. Zeng, X. Zhang, Q. Zhang, X. Gao, J. Mater. Sci. Mater. Electron. **29**, 10362 (2018)
19. J.A. Del-Oso, J.L. Maldonado, G. Ramos-Ortiz, G.M. Rodríguez, M. Güizado-Rodriguez, J. Escalante, B.A. Frontana-Uribe, E. Pérez-Gutiérrez, R. Santillan, Synth. Met. **196**, 83 (2014)
20. Y. Lia, Y. Cao, J. Gao, D. Wang, G. Yu, A.J. Heeger, Synth. Met. **99**, 243 (1999)
21. J. Tauc, R. Grigorovici, A. Vancu, Phys. Status Solidi **15**, 627 (1966)
22. Y. Min, C. Dou, H. Tian, Y. geng, J. Liu, L. Wang, Angew. Chem. Int. Ed. **57**, 2000 (2018)
23. C. Dou, Z. Ding, Z. Zhang, Z. Xie, J. Liu, L. Wang, Angew. Chem. Int. Ed. **54**, 3648 (2015)

24. X. Long, Z. Ding, C. Dou, J. Zhang, J. Liu, L. Wang, Adv. Mater. **28**, 6504 (2016)

25. C. Dou, X. Long, Z. Ding, Z. Xie, J. Liu, L. Wang, Angew. Chem. Int. Ed. **55**, 1436 (2016)

26. M.C. Scharber, D. Mühlbacher, M. Koppe, P. Denk, C. Waldauf, A.J. Heeger, C.J. Brabec, Adv. Mater. **18**, 789 (2006)

27. J. Fischer, D. Ray, H. Kleemann, P. Pahner, M. Schwarze, C. Koerner, K. Vandewal, K. Leo, J. Appl. Phys. **117**, 245501 (2015)

28. Y. Ooyama, Y. Hagiwara, T. Mizumo, Y. Harima, J. Ohshita, RCS Adv. **3**, 18099 (2013)